

Demonstrating Intensity Mapping of Spectral Line Emission from High Redshift Galaxies with Simulated Data

Eli Visbal,^{1,2,*} Hy Trac,^{3,†} and Abraham Loeb^{2,‡}

¹*Jefferson Laboratory of Physics, Harvard University, Cambridge, MA 02138*

²*Harvard-Smithsonian CfA, 60 Garden Street, Cambridge, MA 02138*

³*Department of Physics, Carnegie Mellon University, Pittsburgh, PA 1521*

(Dated: March 29, 2011)

It has been pointed out recently that one can measure the clustering of galaxies by cross correlating the cumulative emission from two different spectral lines which originate from the same sources (Visbal and Loeb 2010). This clustering can be quantified with the line cross power spectrum. By cross correlating the cumulative emission, it is possible to observe galaxies which are too faint to be individually resolved, but which can be detected in clustering due to their large numbers. This technique allows one to study the evolution of a large sample of galaxies which are too faint to be seen individually. In this paper, we test the feasibility of this technique with synthetic data generated from cosmological dark matter simulations. We use a simple prescription to associate galaxies with dark matter halos and create a realization of the light as a function of angle and wavelength over a patch of the sky. This is then used to create synthetic data for two different hypothetical instruments, one aboard the Space Infrared Telescope for Cosmology and Astrophysics (SPICA) and one that consists of a pair of ground based radio telescopes designed to measure the CO(1-0) and CO(2-1) emission lines. We find that the line cross power spectrum can be measured from the synthetic data with errors consistent with the analytical prediction from (Visbal and Loeb 2010). There are two additional complications. First, small k-modes along the line of sight which are contaminated during the foreground removal process must be discarded, slightly increasing the measurement errors on large scales. Additionally, when masking out contaminating emission lines from bright foreground galaxies one must be careful not to introduce a spurious correlation between the data sets being cross correlated.

PACS numbers:

I. INTRODUCTION

Recently, a new method of statistically observing the faintest galaxies has been proposed, namely cross correlating spectral line emission from the same galaxies in different lines. In this way, it is possible to measure the clustering of galaxies which are too faint to be seen individually, but which contribute significantly to the cumulative emission due to their large numbers [1–3].

Atoms and molecules in the interstellar medium of galaxies produce line emission at particular rest frame wavelengths [4]. For galaxies at cosmological distances, this line emission is redshifted by a factor of $(1+z)$ due to the expansion of the universe. Thus, for emission in a particular spectral line, the observed angle on the sky and the observed wavelength correspond to a location in redshift space. With observational data which includes both spectral and spatial information, one can then measure the three dimensional clustering of galaxies.

Before line emission can be associated with a particular location in space, one must isolate it from spectrally extended emission. Galactic continuum emission and spectrally smooth astrophysical foregrounds and backgrounds

(e.g. Cosmic Microwave Background, galactic dust emission) can be removed by fitting smooth functions of frequency to data and subtracting them away (this has been discussed extensively in the context of cosmological 21cm observations [5–9]). After galactic continuum and foreground emission are removed there is still another important issue, confusion from multiple emission lines. With multiple lines of different rest frame wavelengths the intensity at a particular observed frequency corresponds to emission from multiple redshifts, one for each emission line. With both spatial and frequency information, the total emission corresponds to a superposition of the 3D distribution of galaxies at different redshifts.

Fortunately, it is possible to statistically isolate the fluctuations from a particular redshift by cross correlating the emission from two different lines. If one compares the fluctuations at two different wavelengths, which correspond to the same redshift in two different emission lines, the fluctuations will be strongly correlated. However, the signal from any other lines arises from galaxies at different redshifts which are very far apart and thus will have much weaker correlation (see Figure 1). In this way one can measure either the 2-point correlation function or power spectrum of galaxies at some target redshift weighted by the total emission in the spectral lines being cross correlated.

We emphasize that one can measure the line cross power spectrum from galaxies which are too faint to be seen individually over detector noise. Hence, a measure-

*evisbal@fas.harvard.edu

†hytrac@cmu.edu

‡aloeb@cfa.harvard.edu

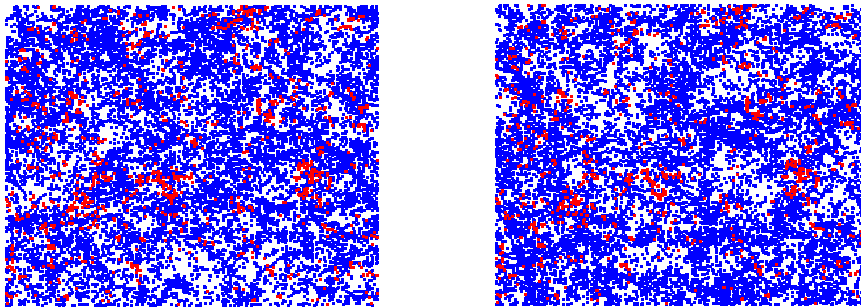


FIG. 1: A slice of our simulated realization of line emission from galaxies at $441\mu\text{m}$ (left) and $364\mu\text{m}$ (right). The slice is 250 comoving Mpc across and has a depth of $\Delta\nu/\nu = 0.001$. The colored squares indicate pixels in our SPICA example (presented below) which have line emission greater than $2 \cdot 10^{-21} \text{erg/s/cm}^2/\text{Hz/Sr}$ for the left panel and $2.5 \cdot 10^{-21} \text{erg/s/cm}^2/\text{Hz/Sr}$ for the right panel. The emission from OI($63\mu\text{m}$) and OIII($52\mu\text{m}$) are shown as red in the left and right plots respectively. These lines come from the same galaxies at $z = 6$. All of the other lines in Table I are included and plotted in blue. If one cross correlates data at these two frequencies the emission in OI and OIII from $z = 6$ will correlate, but the other emission is essentially uncorrelated.

ment of the line cross power spectrum can provide information about the total line emission from all of the galaxies which are too faint to be directly detected. Of course this could be measured at a series of different redshifts in a number of different lines to learn about cosmic galaxy evolution. Changes in the minimum mass of galaxies due to reionization of the intergalactic medium could also potentially be measured.

In this work, we use cosmological simulations to test the feasibility of measuring the galaxy cross power spectrum. We create synthetic data sets for two instruments and then test how well the cross power spectrum can be measured. We find that the cross power spectrum can be measured with uncertainty given by the equation (see Eq. 7 below) derived in [1]. However there are additional complications. Small k-modes along the line of sight which are contaminated during the foreground removal process must be discarded, increasing the uncertainty on large scales. Additionally, when masking out contaminating emission lines from bright foreground galaxies one must be careful not to introduce a spurious correlation between the data sets being cross correlated.

The paper is organized as follows. In §2 we describe the methods used in this paper. This includes a brief review of the galaxy line cross power spectrum, a description of the synthetic data sets, the details of the simulations, and a discussion of the steps involved in measuring the cross power spectrum. In §3 and §4 we present our results for the SPICA example and the CO(1-0) and CO(2-1) telescopes respectively. Finally, we discuss and summarize our conclusions in §5. Throughout, we assume a ΛCDM cosmology with $\Omega_\Lambda = 0.73$, $\Omega_m = 0.27$, $\Omega_b = 0.045$, $h = 0.7$, $n_s = 0.96$ and $\sigma_8 = 0.8$ [10].

II. METHOD

A. Galaxy line cross power spectrum

First, we briefly review the galaxy line cross power spectrum. For a more complete discussion see [1]. We assume that emission is measured both as a function of angle on the sky and observed wavelength. If one fits a smooth function of wavelength in each direction on the sky and subtracts it from the data, ideally one obtains the fluctuations from the average signal as a function of angle and wavelength, $\Delta S(\theta_1, \theta_2, \nu) = S(\theta_1, \theta_2, \nu) - \bar{S}$. These originate from a number of different sources,

$$\Delta S_1 = \Delta S_{\text{line1}} + \Delta S_{\text{noise}} + \Delta S_{\text{badline1}} + \Delta S_{\text{badline2}} + \dots \quad (1)$$

which include contributions from the target galaxies we wish to cross correlate, detector noise, and emission in different lines from galaxies at different redshifts which we refer to as “bad line” emission. There is a one to one correspondence between angular position and wavelength and position in redshift space for emission in a particular line. Thus, we are free to work in comoving coordinates at the location of the target galaxies instead of angle and wavelength. One can cross correlate the fluctuations in two different lines from the same galaxies. We define the line cross correlation function as,

$$\xi_{1,2}(\mathbf{r}) = \langle \Delta S_1(\mathbf{r}_o, \mathbf{x}) \Delta S_2(\mathbf{r}_o, \mathbf{r} + \mathbf{x}) \rangle, \quad (2)$$

where the center of the survey volume is denoted by \mathbf{r}_o .

Because the noise fluctuations in the two different data sets are uncorrelated and galaxies seen in different bad lines will have very large separations and thus be essentially uncorrelated we are only left with contributions from the target galaxies. On large scales we can make the assumption that line fluctuations due to galaxy clustering are given by $\Delta S = \bar{S} \delta(\mathbf{r})$, where \bar{S} is the average

line signal, \bar{b} is the luminosity weighted average galaxy bias, and $\delta(\mathbf{r})$ is the cosmological over-density at a location \mathbf{r} . It follows that,

$$\begin{aligned} \xi_{1,2}(\mathbf{r}) &= \langle \Delta S_{\text{line}1}(\mathbf{r}_o, \mathbf{x}) \Delta S_{\text{line}2}(\mathbf{r}_o, \mathbf{r} + \mathbf{x}) \rangle \\ &= \bar{S}_1 \bar{S}_2 \bar{b}^2 \langle \delta(\mathbf{x}) \delta(\mathbf{r} + \mathbf{x}) \rangle = \bar{S}_1 \bar{S}_2 \bar{b}^2 \xi(\mathbf{r}), \end{aligned} \quad (3)$$

where $\xi(\mathbf{r})$ is the cosmological matter correlation function and the subscript numbers denote the different lines being cross correlated.

The line cross power spectrum is then defined as the Fourier transform,

$$P_{1,2}(\mathbf{k}) = \int d^3\mathbf{r} \xi_{1,2}(\mathbf{r}) e^{i\mathbf{k}\cdot\mathbf{r}} = \bar{S}_1 \bar{S}_2 \bar{b}^2 P(\mathbf{k}) + P_{\text{shot}}, \quad (4)$$

where P_{shot} is the shot-noise power spectrum due to the discrete nature of galaxies.

An unbiased estimator for the cross power spectrum is given by the product of the Fourier transforms of the data sets,

$$\hat{P}_{1,2} = \frac{V}{2} (f_{\mathbf{k}}^{(1)} f_{\mathbf{k}}^{(2)*} + f_{\mathbf{k}}^{(1)*} f_{\mathbf{k}}^{(2)}), \quad (5)$$

where V is the volume of the survey and the superscripts denote the different lines being cross correlated. The Fourier amplitude is given by,

$$f_{\mathbf{k}} = \int d^3\mathbf{r} \Delta S(\mathbf{r}_o, \mathbf{r}) W(\mathbf{r}) e^{i\mathbf{k}\cdot\mathbf{r}}. \quad (6)$$

Here $W(\mathbf{r})$ is a window function that is constant over the survey volume and zero at all other locations. It is normalized such that, $\int W(\mathbf{r}) d^3\mathbf{r} = 1$.

The root mean square error in a measurement of the cross power spectrum at one particular \mathbf{k} value is given by,

$$\delta P_{1,2}^2 = \frac{1}{2} (P_{1,2}^2 + P_{1\text{total}} P_{2\text{total}}), \quad (7)$$

where $P_{1\text{total}}$ and $P_{2\text{total}}$ are the total power spectrum corresponding to the first line and second line being cross correlated. Each of these includes a term for the power spectrum for each of the bad lines, the target line, and detector noise (see Appendix A of [1]). When averaging nearby values of the power spectrum this error goes down by a factor of $\sqrt{N_{\text{modes}}}$, where N_{modes} is the number of statistically independent \mathbf{k} -values at which the power spectrum is measured.

B. Synthetic data set

In order to test the feasibility of measuring the line cross power spectrum we create synthetic data sets for instruments measuring both spatial and spectral information. Our goal is to produce a realization of the light from all galaxies as a function of angle and observed

wavelength on a patch of the sky. We create these data with a cosmological dark matter simulation (described in detail below). From the simulation we construct a light cone which has the distribution of dark matter which would be observed today in the volume corresponding to an angular patch on the sky out to a redshift of $z = 10$.

We use a simple prescription to populate the dark matter light cone with galaxies. We assume that galaxies are found in dark matter halos above a minimum mass, M_{min} . Before reionization M_{min} is set by the requirement that gas can cool efficiently via atomic hydrogen cooling, corresponding to halos with virial temperatures greater than 10^4K , whereas after reionization this is the threshold for assembling heated gas out of the photo-ionized intergalactic medium, corresponding to a minimum virial temperature of 10^5K [11–18].

After associating galaxies with dark matter halos in the simulation we produce a spectrum for each galaxy. To do this we assume that both line and continuum emission are proportional to the star formation rate of the galaxy, which we estimate with a simple prescription. For the continuum, we take the measured spectral energy distribution of M82 and scale it with the star formation rate (SFR) of each galaxy. Although we assign each galaxy a continuum our results are completely insensitive to this, as it is removed in the fitting and subtraction stage of data analysis discussed below.

In order to estimate the amplitude of line emission fluctuations we assume a linear relationship between line luminosity, L , and star formation rate, M_* . The line luminosity from a galaxy is then given by $L = \dot{M}_* \cdot R$, where R is the ratio between star formation rate and line luminosity for a particular line. This is similar to existing relations in different bands (see [19]) and was used in the past to estimate the strength of the galactic lines [20]. The values for relevant lines are shown in Table I. For the first 7 lines, we use the same ratios, R , as [20] which were calculated by taking the geometric average of the ratios from an observational sample of lower redshift galaxies [21]. The other lines have been calibrated based on the galaxy M82. We assign a width to the lines based on the rotational velocity of the dark matter halos, but for the spectral resolutions we consider in our examples the results are mostly insensitive to this. This is because the majority of the signal comes from lines which are spectrally unresolved.

We use observed UV luminosity functions of galaxies to calibrate the SFR assigned to dark matter halos with a simple abundance matching technique. With the luminosity functions we determine the number density of galaxies as a function of SFR with the relation

$$L_{\text{UV}} = \text{const} \frac{\text{SFR}}{M_{\odot} \text{yr}^{-1}} \text{ergs/s/Hz}, \quad (8)$$

where const is given by $8 \cdot 10^{27}$ at 1500\AA . This assumes a Salpeter initial mass function from $0.1 - 125 M_{\odot}$ and constant SFR $\gtrsim 100\text{Myr}$. The relationship between halo mass and SFR_{*i*} at some particular mass, M_i is then found

TABLE I: Assumed ratio between star formation rate, \dot{M}_* , and line luminosity, L , for various lines. For the first 7 lines this ratio is measured from a sample of low redshift galaxies. The other lines have been calibrated based on the galaxy M82. We obtain the luminosity in a line from: $L[L_\odot] = R \cdot \dot{M}_*[M_\odot \text{ yr}^{-1}]$.

Species	Emission Wavelength[μm]	R[$L_\odot/(M_\odot/\text{yr})$]
CII	158	6.0×10^6
OI	145	3.3×10^5
NII	122	7.9×10^5
OIII	88	2.3×10^6
OI	63	3.8×10^6
NIII	57	2.4×10^6
OIII	52	3.0×10^6
$^{12}\text{CO}(1-0)$	2610	3.7×10^3
$^{12}\text{CO}(2-1)$	1300	2.8×10^4
$^{12}\text{CO}(3-2)$	866	7.0×10^4
$^{12}\text{CO}(4-3)$	651	9.7×10^4
$^{12}\text{CO}(5-4)$	521	9.6×10^4
$^{12}\text{CO}(6-5)$	434	9.5×10^4
$^{12}\text{CO}(7-6)$	372	8.9×10^4
$^{12}\text{CO}(8-7)$	325	7.7×10^4
$^{12}\text{CO}(9-8)$	289	6.9×10^4
$^{12}\text{CO}(10-9)$	260	5.3×10^4
$^{12}\text{CO}(11-10)$	237	3.8×10^4
$^{12}\text{CO}(12-11)$	217	2.6×10^4
$^{12}\text{CO}(13-12)$	200	1.4×10^4
CI	610	1.4×10^4
CI	371	4.8×10^4
NII	205	2.5×10^5
$^{13}\text{CO}(5-4)$	544	3900
$^{13}\text{CO}(7-6)$	389	3200
$^{13}\text{CO}(8-7)$	340	2700
HCN(6-5)	564	2100

from the relation $n_h(M > M_i) = n_g(\text{SFR} > \text{SFR}_i)$. Here $n_h(M)$ is the number density of dark matter halos above mass M in our simulation and $n_g(\text{SFR})$ is the number density of galaxies implied by the UV luminosity function above star formation rate SFR. This procedure is carried out in a number of different redshift bins which cover our entire light cone. As a simple correction for attenuation due to dust we increase the SFR of all halos in each redshift bin by a factor which sets the global SFR equal to the blue solid curve in Figure 10 of [22]. The particular parameters used for the abundance matching procedure are listed in Table II.

The largest dark matter halos in our simulation may host multiple galaxies. To incorporate this effect in our synthetic data we have used a simple prescription for the halo occupation distribution. Following the work of [26] for the distribution of dark matter sub-halos, we consider two different types of galaxies, central and satellite. We

TABLE II: UV Luminosity Function Schechter function parameters used for abundance matching to assign SFR to dark matter halos.

z	$\phi^*(\times 10^{-3} \text{Mpc}^{-3})$	M_{AB}^*	α	Ref.
0.-0.5	4.07	-18.05	-1.21	[23]
0.5-1.0	3.0	-19.17	-1.52	[24]
1.0-1.5	1.26	-20.08	-1.84	[24]
1.5-2.0	2.3	-20.17	-1.60	[24]
2.0-2.7	2.75	-20.7	-1.73	[22]
2.7-3.4	1.71	-20.97	-1.73	[22]
3.4-4.5	1.3	-20.98	-1.73	[25]
4.5-5.5	1.0	-20.64	-1.66	[25]
5.5-6.5	1.4	-20.24	-1.74	[25]
6.5-10.5	1.4	-19.3	-1.74	[25]

assume that the distribution of central galaxies is a step function with mass. Above M_{min} , given by the requirement that galaxies can be assembled from photoionized gas in the IGM ($T_{\text{vir}} = 10^5$), we assume each halo has one galaxy at its center. We then assume that there are a number of satellite galaxies given by a Poisson distribution with a mean of $N_{\text{sat}} = (M/M_1)^\beta$, with $\beta = 1$, and $M_1 = 30M_{\text{min}}$ at $z = 0 - 0.5$, $M_1 = 20M_{\text{min}}$ at $z = 0.5 - 2$, and $M_1 = 10M_{\text{min}}$ at $z > 2$. We distribute these galaxies randomly, but weighted by an NFW profile, throughout the larger host dark matter halo. We treat the central and satellite galaxies as different halos in order to perform the abundance matching procedure described above. We assign half of the total halo mass to the central galaxy halos and assign the remainder of the mass equally to all of the satellite galaxy halos.

To create our data set we then assign an angular and spectral resolution and pixelate the signal from the galaxies in the corresponding three dimensional data cube. Finally, we add detector noise and bright astronomical foreground and background emission. For the examples below we include both the CMB and emission from dust in our galaxy. The dust emission is treated as a black body with a frequency squared emissivity scaled to match the background radiation measured by COBE FIRAS in the faintest area on the sky [27]. In Figure 2, we illustrate the different components which make up our data sets.

C. Simulations

Fill in later.

D. Cross power spectrum measurement

Measuring the cross power spectrum consists of three main steps:

1. Fitting a smooth function of wavelength to each pixel and subtracting it away.

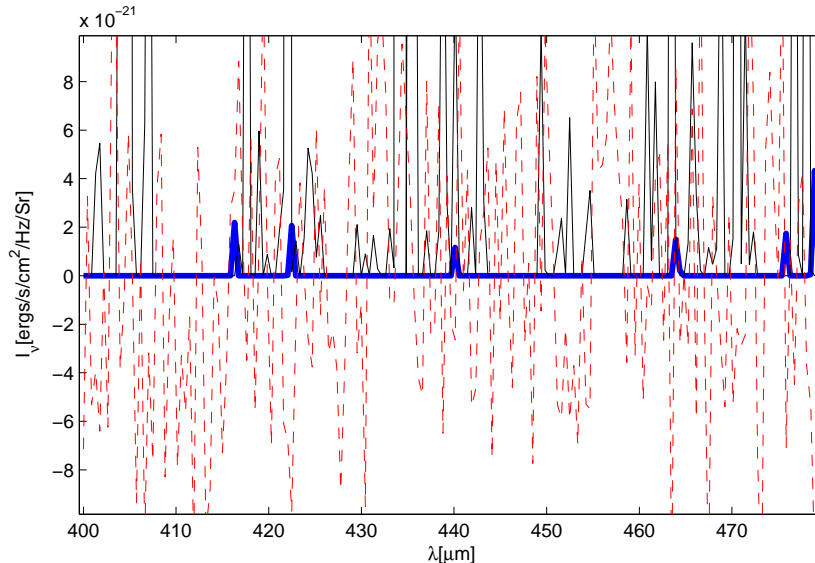


FIG. 2: Various components of the synthetic data set for a typical line of sight. We plot data from the SPICA example discussed below. The thick blue curve is the line emission from the target galaxies, the thin red dashed curve is the contribution from detector noise, and the thin black curve is the emission from all of the bad lines. We have not included the bright astrophysical foregrounds (dominated by dust emission at these wavelengths), because they are orders of magnitude greater than all of the components plotted here. This emission along with galaxy continuum (not plotted) is removed in the fitting and subtraction step of measuring the power spectrum discussed below.

2. Masking out the brightest voxels (note that we term each line of sight on the sky a pixel and each spectral component of the 3D data cube a voxel).

3. Taking the product of the Fourier modes to estimate the power spectrum and then averaging in spherical shells in k -space.

We discuss these in turn. The fitting stage is necessary because we only seek to measure the signal coming from line emission and our data contains signal from both galaxy continuum emission as well as bright astrophysical foregrounds and backgrounds. Since these other sources vary slowly in the spectral direction we can remove them by fitting a smooth function of wavelength to each pixel on the sky and subtracting it. This is the same procedure which has been discussed extensively in the context of cosmological measurements of 21cm radiation from neutral hydrogen [5–9].

More specifically, with our data sets we fit a polynomial in wavelength to the spectrum in each pixel and then subtract it away. It is inevitable to fit to the line signal on large scales and subtract some of it away. In order to minimize this effect we do not include voxels in our fit which contain line emission greater than five times the RMS fluctuations due to detector noise. We do this by an iterative fit. We fit once to remove the bright foregrounds and identify the bright voxels and then fit again excluding them.

There will necessarily be some signal lost as a result of the fitting and subtraction stage. Luckily as discussed in [5], if we decompose our signal into Fourier modes,

the lost signal is from small k -modes (corresponding to long wavelengths) along the line of sight. If we exclude these corrupted k -modes in step 3 of measuring the cross power spectrum described below we still have an unbiased estimation of the cross power spectrum without subtraction losses. Note that throwing away the low k -modes does have a price. Since there are fewer statistical samples of these modes this procedure increases the variance of power spectrum measurements on these scales. Because we wish to minimize the number of these corrupted modes, we fit with the lowest order polynomial which leaves no significant residual foregrounds.

After we have subtracted away the foreground and continuum emission it is necessary to remove the bright remaining voxels. This is necessary because even though line emission from bright foreground galaxies does not bias our measurements of the power spectrum it does greatly increase the error of our measurements.

The masking procedure must be done carefully in order to not introduce spurious correlations between the two data sets being cross correlated. For example, if one simply sets all voxels above some threshold signal equal to zero a spurious change to the cross power spectrum is introduced (see Fig. 5). This is because the location of the brightest voxels (mainly due to contaminating bright foreground galaxies) are correlated with the distribution of target line emission. The signal from the bad lines and the target lines overlap so that bright bad lines which appear in the data at locations of over-densities in the target lines are more likely to be above the removal threshold.

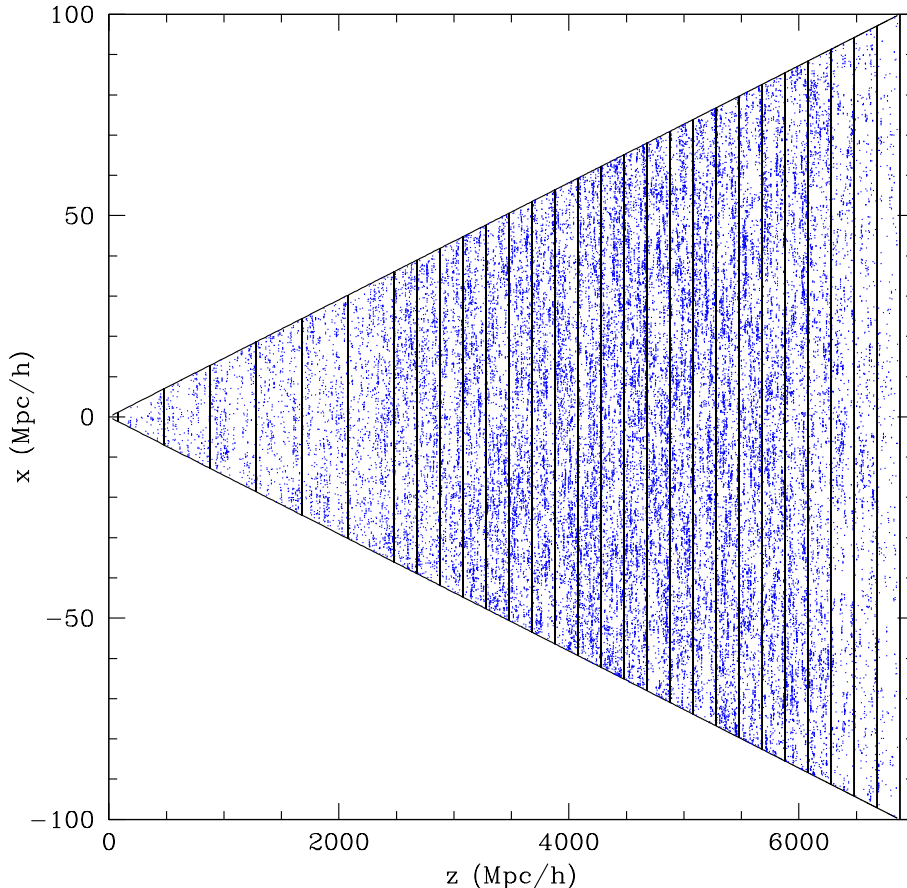


FIG. 3: The light cone used to generate our synthetic data sets.

Thus, the bad lines left after masking in one data cube will be anti-correlated with the target lines in the other cube. This causes the measured cross power spectrum to be lower than what would be measured from the target lines alone.

In order to avoid this type of complication one can mask out voxels in a way which is uncorrelated with the target line emission being measured. This can be done by identifying individual bright sources instead of just removing the brightest voxels in the data. The voxels with bright contaminating lines can then be set to zero. These sources could be identified by looking at a series of different wavelengths and identifying with multiple lines. Entirely different surveys could also be used to determine where contaminating lines from bright foreground galaxies will appear and be removed. In our examples below, we assume that all of the galaxies which emit lines brighter than five times the RMS detector noise can be identified directly. When setting the masked pixels to zero we treat this as a change in the window function, $W(\mathbf{r})$, which appears in Eq. 6. We normalize this new window function such that $\int W(\mathbf{r})d^3\mathbf{r} = 1$ which effectively accounts for the signal we are cross correlating

which happens to be removed with the masking.

In the final step, we take the discrete Fourier transform of the two 3D data cubes being cross correlated. The estimation of the power spectrum at some particular k value is then given by the real part of the product of the survey volume, the Fourier mode of one data set, and the complex conjugate of the same Fourier mode in the other data set. This is equivalent to Eq. (5). Finally, we break k -space into spherical shells with uniform thickness in $\log(k)$. We then take the average estimated power spectrum of all the modes contained within each shell. As discussed above, we do not include short k -modes along the line of sight which have been contaminated during the fitting and subtraction stage. Specifically, we do not include k -modes which have a component along the line of sight less than, k_{cut} , the lowest value for which there is no significant contamination. In the examples below we find that for $k_{\text{cut}} = 0.03$ that there is no significant loss of power due to the foreground removal process.

III. SPICA

A. Instrument

We consider two different examples of instruments and lines which could be used to measure the galaxy line cross power spectrum. In our first example, we use the hypothetical future instrument discussed in [1]. This example illustrates how well a space-borne sub-mm instrument with noise limited by astrophysical backgrounds could perform for the technique discussed in this paper.

We envision an instrument on the Space Infrared Telescope for Cosmology and Astrophysics (SPICA) [28]. SPICA is a 3.5 meter space-borne infrared telescope planned for launch in 2017. It will be cooled below 5K, providing measurements which are orders of magnitude more sensitive than those from current instruments.

We consider an instrument based on the proposed high performance spectrometer μ -spec (H. Moseley, private communication 2009). This instrument will provide background limited sensitivity with wavelength coverage from $250 - 700\mu m$. A number of μ -spec units will be combined to record both angle and spectral data in each pointing, which will be perfectly suited for the cross correlation technique. We assume that spectra for 100 diffraction limited beams can be measured simultaneously with a resolving power of $R = \nu/\Delta\nu = 1000$.

B. Results

We use the simulation described above to create a synthetic data set and measure the cross power spectrum for the example discussed in [1]. We cross correlate OI(63 μm) and OIII(52 μm) from galaxies at a redshift of $z = 6$. We assume the data covers a square on the sky which is 1.7 degrees across (corresponding to 250 Mpc) and a redshift range of $\Delta z = 0.6$ (corresponding 280 Mpc). We assume a total integration time of $2 \cdot 10^6$ seconds spread uniformly across this survey volume. We find an average signal in our data set of $2 \cdot 10^{-22}$ ergs/s/cm²/Hz/Sr for both OI(63 μm) and OIII(52 μm).

In Figure 4, we show that using the procedure described above we can accurately measure the cross power spectrum. We show both the cross power spectrum of the emission from the target lines alone as well as that which is recovered when bad lines, detector noise, and foregrounds are included. The error in measuring the power spectrum is consistent with Eq. 7 derived in [1].

In Figure 5, we show the effects on the measured cross power spectrum of masking out all bright pixels. We have plotted the power spectrum from the target lines alone and also with the bad lines using the same mask in both cases. Clearly the anti-correlation between the masked bad lines and the target lines in the other data set described above have reduce the cross power spectrum.

We find that increasing the sky coverage (i.e. shorter integrations for each patch of the sky, but wider) in-

creases our errors in the power spectrum. This is due to our assumptions about masking bright bad lines. As we go wider the detector noise goes up and the increased number of bright bad lines which are not masked increases the errors on the power spectrum. One would not want to go much deeper over a smaller patch of sky than we consider, because we are already masking roughly 10% of the voxels and masking many more would not enable a reliable Fourier transform.

If the mask were not dependant on the intergration time (i.e. obtained from a different survey of foreground galaxies) it is straight forward to determine in a given time what the optimal sky coverage is for measuring power on a particular scale. Minimizing Eq. 7 with respect to time integrated per patch, holding the total observation time fixed, one finds that the optimal coverage sets $P_{\text{noise1}}P_{\text{noise2}} = P_{1,2}^2 + (P_{1\text{total}} - P_{\text{noise1}})(P_{2\text{total}} - P_{\text{noise2}})$. The product of the detector noise power spectra equals the sum of the sample variance contribution to the power spectrum uncertainty.

IV. INTENSITY MAPPING CO(1-0) AND CO(2-1)

As another example we consider intensity mapping the cross correlations between CO(1-0) and CO(2-1) at high redshifts with a dedicated instrument currently being planned (private communication Judd Bowman 2011). This observation consists of two telescopes: a 20 meter dish and a 10 meter dish to observe CO(1-0) and CO(2-1) respectively. Each of these telescopes can simultaneously observe 3 deg² of the sky with angular resolution set by the beam size (3.5-5 arcmin at $z = 7 - 10$). We assume a spectral resolution of $R = \nu/\Delta\nu = 1000$. While the actual instrument will have a higher resolution this is sufficient to measure fluctuations on the scales we consider. To determine the detector noise we use the radiometer equation

$$\sigma_T = \frac{T_{\text{sys}}}{\sqrt{2t\Delta\nu}}, \quad (9)$$

where T_{sys} is the system temperature which we have assumed to be 30K, t is the integration time which we have assumed is $3 \cdot 10^7$ s, and the factor of $\sqrt{2}$ appears in the denominator because the intensity will be mapped from dual polarization. We create a synthetic data set for this instrument centered at $z = 7.5$ and the recovered cross power spectrum is shown in Figure 6. We find an average line emission signal in both lines to be $0.06\mu K$.

V. DISCUSSION AND CONCLUSIONS

It has been pointed out that, by cross correlating emission in different spectral lines from the same galaxies, it is possible to measure their clustering. This clustering, quantified by the line cross power spectrum, can be

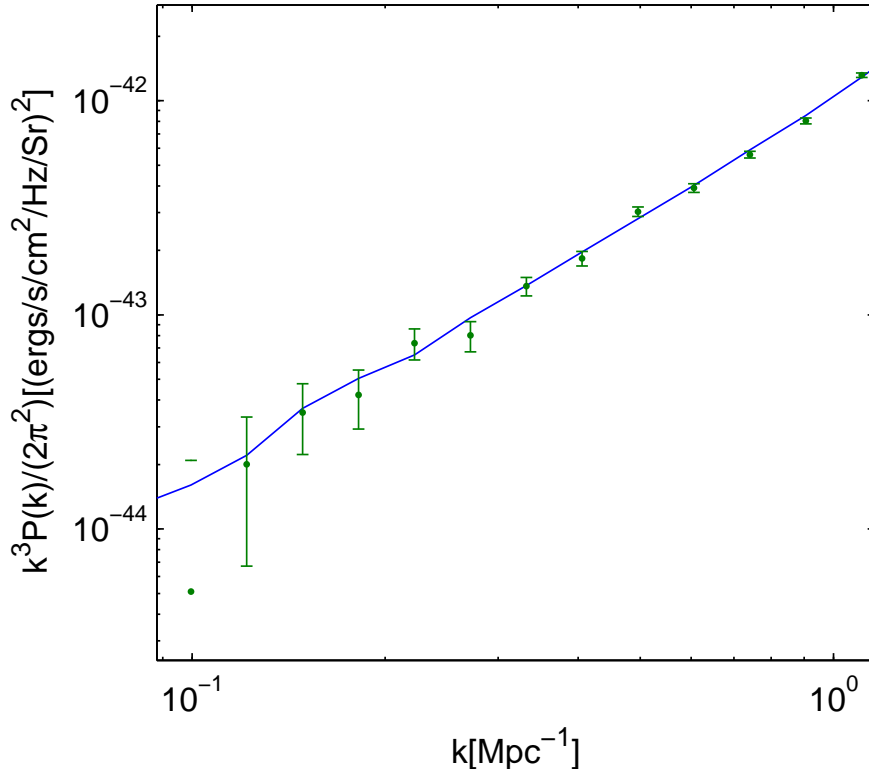


FIG. 4: The cross power spectrum of OI($63 \mu\text{m}$) and OIII($52 \mu\text{m}$) at $z = 6$ measured from simulated data for our hypothetical instrument modeled after SPICA. The blue curve is the cross power spectrum measured when only line emission from galaxies in the target lines are included. The green points are the recovered power spectrum when detector noise, bad line emission, galaxy continuum emission, and bright astrophysical foreground and background emission (i.e. dust in our galaxy and the CMB) are included. The error bars are the theoretical prediction of the root mean square error derived in [1] and given by Eq. 7. In determining the error bars we have estimated $P_{1\text{total}}$ and $P_{2\text{total}}$ using our simulated data.

measured for galaxies which are too faint to detect individually, but which can be observed in aggregate due to their large numbers [1]. It is necessary to cross correlate different lines, because this removes the contamination caused by bad lines, emission in other lines from either foreground or background galaxies.

In this paper, we have shown that the line cross power spectrum can be accurately measured from synthetic data sets which were created using cosmological dark matter simulations. To produce our synthetic data, we associate dark matter halos with galaxies and assign each a spectrum. The continuum is generated by scaling that of M82 with the star formation rate in each halo and line emission is set by calibrating with lower redshift galaxies. The star formation rate is computed for halos with an abundance matching technique calibrated to observation of the UV galaxy luminosity functions. Our synthetic data also include detector noise and bright emission due to astrophysical foregrounds and backgrounds such as that from dust in our galaxy and the CMB. Even if our simple prescription deviates somewhat from reality, it still illustrates our main point, that whatever the underlying power spectrum of emission from galaxies is it

can be measured with the accuracy predicted analytically by Eq. 7.

Measuring the line cross power spectrum consists of three main steps. First, a smooth function such as a polynomial is fit to each pixel on the sky and subtracted from the data to remove smooth foregrounds and the continuum emission from galaxies. Next, bright voxels are masked out. One must be careful in the masking technique as it is possible to introduce spurious correlations if the masks are correlated with the target lines which appear in both data cubes. This can be avoided if bright sources are found individually at high significance and the corresponding voxels with bright contaminating lines are set to zero. Finally, the data is Fourier transformed and then the power spectrum is averaged in spherical shells. Modes corresponding to long wavelengths along the line of sight are not included, because they are contaminated during the fitting and subtraction step.

We find that the line cross power spectrum is measured with the accuracy predicted analytically in Eq. 7, derived in [1]. In particular, we tested two hypothetical instruments, a space-borne telescope mounted on SPICA and a pair of large ground based telescopes designed to measure

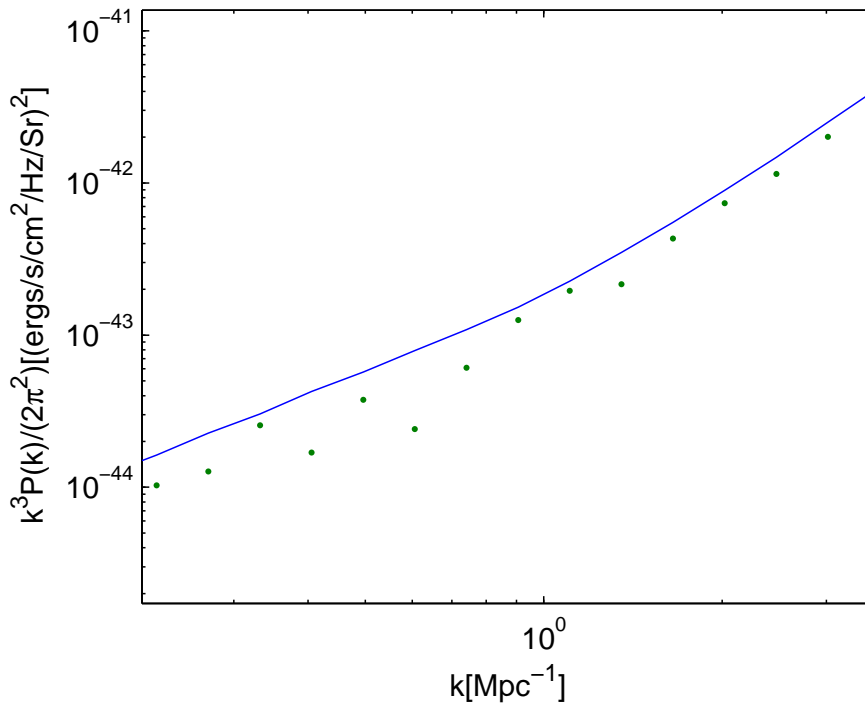


FIG. 5: The measured power spectrum when masking is done by simply setting the fluctuations in all voxels with signal greater than five times the RMS detector noise to zero. We use the same instrumental and survey parameters as in Figure 4. The points plotted are the measurements of the cross power spectrum after all bright pixels have been masked and set to zero. The line is the power spectrum if only the target galaxy lines are included (but using the same mask). Clearly the anti-correlation between the masked bad lines and the good lines in opposite cubes produces a systematic shift in the power spectrum.

the emission of CO(1-0) and CO(2-1). These would be very interesting observations to carry out because they

could reveal details about the evolution of faint galaxies which cannot be directly measured in large numbers.

-
- [1] E. Visbal and A. Loeb, **11**, 16 (2010), 1008.3178.
[2] Y. Gong, A. Cooray, M. B. Silva, M. G. Santos, and P. Lubin, **728**, L46+ (2011), 1101.2892.
[3] C. L. Carilli, **730**, L30+ (2011), 1102.0745.
[4] J. Binney and M. Merrifield, *Galactic astronomy* (Princeton University Press, 1998).
[5] N. Petrovic and S. P. Oh, ArXiv e-prints (2010), 1010.4109.
[6] M. F. Morales, *Astrophys. J.* **619**, 678 (2005).
[7] X.-M. Wang, M. Tegmark, M. Santos, and L. Knox, *Astrophys. J.* **650**, 529 (2006).
[8] M. McQuinn, O. Zahn, M. Zaldarriaga, L. Hernquist, and S. R. Furlanetto, *Astrophys. J.* **653**, 815 (2006).
[9] A. Liu, M. Tegmark, J. Bowman, J. Hewitt, and M. Zaldarriaga, *Mon. Not. Roy. Astron. Soc.* **398**, 401 (2009), arXiv:astro-ph/0903.4890.
[10] E. Komatsu, K. M. Smith, J. Dunkley, C. L. Bennett, B. Gold, G. Hinshaw, N. Jarosik, D. Larson, M. R.olta, L. Page, et al., ArXiv e-prints (2010), arXiv:astro-ph/1001.4538.
[11] A. Mesinger and M. Dijkstra, *Mon. Not. Roy. Astron. Soc.* **390**, 1071 (2008).
[12] G. Efstathiou, *Mon. Not. Roy. Astron. Soc.* **256**, 43P (1992).
[13] A. A. Thoul and D. H. Weinberg, *Astrophys. J.* **465**, 608 (1996).
[14] L. Hui and N. Y. Gnedin, "Mon. Not. Roy. Astron. Soc." **292**, 27 (1997).
[15] S. Wyithe and A. Loeb, *Nature* **441**, 332 (2006).
[16] P. R. Shapiro, M. L. Giroux, and A. Babul, *Astrophys. J.* **427**, 25 (1994).
[17] D. Babich and A. Loeb, *Astrophys. J.* **640**, 1 (2006), arXiv:astro-ph/0509784.
[18] Z. Haiman, M. J. Rees, and A. Loeb, *Astrophys. J.* **476**, 458 (1997), arXiv:astro-ph/9608130.
[19] R. C. Kennicutt, Jr., *Annual Review of Astronomy and Astrophysics* **36**, 189 (1998), arXiv:astro-ph/9807187.
[20] M. Righi, C. Hernández-Monteaquedo, and R. A. Sunyaev, *Astronomy and Astrophysics* **489**, 489 (2008), arXiv:astro-ph/0805.2174.
[21] S. Malhotra, M. J. Kaufman, D. Hollenbach, G. Helou, R. H. Rubin, J. Brauher, D. Dale, N. Y. Lu, S. Lord, G. Stacey, et al., *Astrophys. J.* **561**, 766 (2001), arXiv:astro-ph/0106485.

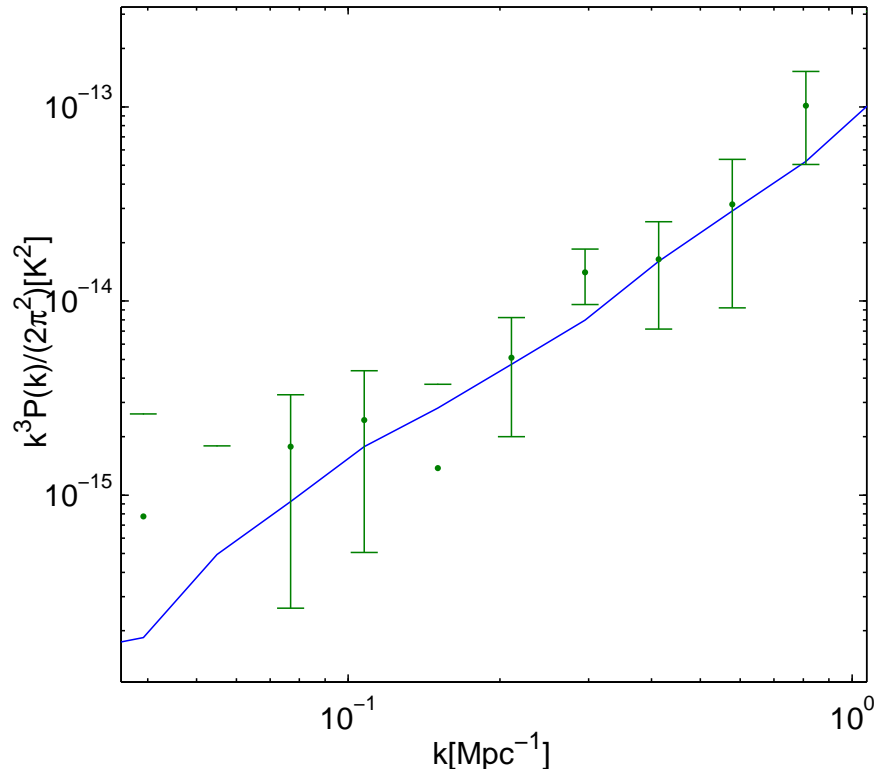


FIG. 6: The cross power spectrum of CO(1-0) and CO(2-1) from a central redshift of $z = 7.5$ measured with the telescope described in §4. An integration of $3 \cdot 10^7$ and a redshift range of $\Delta z = 0.9$ are assumed. The solid blue line is the power spectrum of the CO line emission alone measured from our simulated data. The green are the measurements of the power spectrum after detector noise and bad line emission from the other lines in Table I are included. The error bars are calculated from Eq. 7, where we have estimated $P_{1\text{total}}$ and $P_{2\text{total}}$ using our simulated data.

- [22] N. A. Reddy and C. C. Steidel, *Astrophys. J.* **692**, 778 (2009), 0810.2788.
- [23] S. Arnouts, D. Schiminovich, O. Ilbert, L. Tresse, B. Milliard, M. Treyer, S. Bardelli, T. Budavari, T. K. Wyder, E. Zucca, et al., **619**, L43 (2005), arXiv:astro-ph/0411391.
- [24] P. A. Oesch, R. J. Bouwens, C. M. Carollo, G. D. Illingworth, D. Magee, M. Trenti, M. Stiavelli, M. Franx, I. Labbé, and P. G. van Dokkum, **725**, L150 (2010), 1005.1661.
- [25] R. J. Bouwens, G. D. Illingworth, M. Franx, and H. Ford, *Astrophys. J.* **670**, 928 (2007), 0707.2080.
- [26] A. V. Kravtsov, A. A. Berlind, R. H. Wechsler, A. A. Klypin, S. Gottlöber, B. Allgood, and J. R. Primack, *Astrophys. J.* **609**, 35 (2004), arXiv:astro-ph/0308519.
- [27] D. J. Fixsen, E. Dwek, J. C. Mather, C. L. Bennett, and R. A. Shafer, *Astrophys. J.* **508**, 123 (1998), arXiv:astro-ph/9803021.
- [28] B. Swinyard, T. Nakagawa, P. Merken, P. Royer, T. Souverijns, B. Vandenbussche, C. Waelkens, P. Davis, J. Di Francesco, M. Halpern, et al., *Experimental Astronomy* **23**, 193 (2009).